Journal of Mathematical Modeling
Vol. 12, No. 3, 2024, pp. 501–516. Research Article

JMM

A uniformly convergent numerical scheme for singularly perturbed parabolic turning point problem

Sisay Ketema Tesfaye[†*], Gemechis File Duressa[‡], Mesfin Mekuria Woldaregay[†], Tekle Gemechu Dinka[†]

[†]*Department of Applied Mathematics, Adama Science and Technology University, Adama, Ethiopia*
[‡]*Department of Mathematics, Jimma University, Jimma, Ethiopia*
Email(s): sisayk12@gmail.com, gemechis.file@ju.edu.et, mesfinmekuria@astu.edu.et, tekgem@yahoo.com

Abstract. A uniformly convergent numerical scheme is developed for solving a singularly perturbed parabolic turning point problem. The properties of continuous solutions and the bounds of the derivatives are discussed. Due to the presence of a small parameter as a multiple of the diffusion coefficient, it causes computational difficulty when applying classical numerical methods. As a result, the scheme is formulated using the Crank-Nicolson method in the temporal discretization and an exponentially fitted finite difference method in the space on a uniform mesh. The existence of a unique discrete solution is guaranteed by the comparison principle. The stability and convergence analysis of the method are investigated. Two numerical examples are considered to validate the applicability of the scheme. The numerical results are displayed in tables and graphs to support the theoretical findings. The scheme converges uniformly with order one in space and two in time.

Keywords: Turning point problem, fitting factor, finite difference method, uniform convergence.
AMS Subject Classification 2010: 65M06, 65M12, 65M15.

1 Introduction

We consider a degenerate convection-diffusion problem of the form

$$\begin{cases} \mathscr{L}z(s,t) \equiv \varepsilon z_{ss}(s,t) + a(s)z_s(s,t) - b(s,t)z_t(s,t) - e(s,t)z(s,t) = g(s,t), \\ (s,t) \in D = (0,1) \times (0,T], \\ z(s,t) = \psi_b(s,t),\ (s,t) \in \eta_b := [0,1] \times \{0\}, \\ z(0,t) = \psi_l(t),\ (s,t) \in \eta_l := \{0\} \times [0,T], \\ z(1,t) = \psi_r(t),\ (s,t) \in \eta_r := \{1\} \times [0,T], \end{cases} \tag{1}$$

*Corresponding author
Received: 8 February 2024 / Revised: 10 May 2024 / Accepted: 12 May 2024
DOI: 10.22124/JMM.2024.26669.2349

where $a(s) = a_0(s)s^p,\ a_0(s) \geq \alpha > 0,\ s \in [0,1],\ p \geq 1$, and the perturbation parameter $\varepsilon \in (0,1]$.

The functions $a(s), b(s,t), e(s,t), g(s,t)$ on $\bar{D}$, and $\psi_b(s,t), \psi_l(t), \psi_r(t)$ on $\eta = \eta_b \cup \eta_l \cup \eta_r = \bar{D} - D$ are assumed to be sufficiently smooth and bounded that carry out the assumptions $0 \leq a(s),\ 0 < \beta \leq b(s,t),\ 0 < \gamma \leq e(s,t),\ (s,t) \in \bar{D} = [0,1] \times [0,T]$ for some fixed $T > 0$. The coefficient of convection term $a(s)$ of (1) vanishes at $s = 0$, i.e., $a(0) = 0$. Such a problem is known as a turning point problem. When the convection coefficient equals zero, the problem presents either a boundary or an interior turning point. A boundary turning point arises when the convection coefficient equals zero at the boundary, while an interior turning point occurs when it equals zero within the domain [7]. For $p = 1$, problem (1) is a simple turning point problem, whereas for $p > 1$, it becomes a multiple turning point problem [4,10]. The problem of simple turning point finds extensive applications in modeling heat flow and mass transport near an oceanic rise, owing to a linear velocity distribution [6]. On the other hand, the multiple turning point problem pertains to thermal boundary layers in laminar flow for high-velocity distribution [19]. Generally, the solution of the problem described in (1) exhibits a parabolic boundary layer of width $O(\sqrt{\varepsilon})$, in the vicinity of the left boundary layer as ε approaches zero.

It has been observed that the presence of a particular boundary layer can hinder the effectiveness of traditional numerical methods. To overcome this computational difficulty, developing suitable numerical methods has received remarkable attention from researchers. Several works have been done to solve problem (1). For instance, Dunne et al. [3] proposed an upwind scheme using a piecewise uniform mesh in space and the backward Euler scheme in time, which is almost first-order accurate in space and first-order accurate in time. Gupta et al. [5] developed a B-spline collocation method on a piecewise uniform mesh in space, along with an implicit Euler method in time. They have achieved an order of accuracy almost second-order in space and first-order in time. In [11], Sahoo and Gupta applied a numerical scheme that combined the implicit Euler and a simple upwind scheme on a piecewise uniform mesh. Using the Richardson extrapolation technique in both space and time directions, they enhanced the order of accuracy to almost second-order in space and second-order in time.

In [12], a classical finite difference scheme on a Shishkin mesh and backward Euler was suggested, and by applying the Richardson extrapolation technique, the order of accuracy was enhanced to almost second-order in space and second-order in time. In [13], a hybrid method combining the central difference method and the midpoint upwind scheme on a piecewise uniform Shishkin mesh was applied and obtained almost second-order accuracy in space and first-order in time. In [10], an upwind scheme was employed on a layer adaptive non-uniform mesh in the spatial variable and the implicit Euler scheme in the time, and obtained first-order accuracy in both space and time.

Singh et al. [17] suggested a quadratic spline collocation method on an exponentially graded mesh in the space and the Crank-Nicolson method in time, and second-order accuracy in both space and time was achieved. In [22], a hybrid scheme was developed for an interior layer problem by combining the central difference method and midpoint upwind scheme on a piecewise uniform Shishkin mesh in space and backward Euler in time and improved the time accuracy to second-order by using Richardson extrapolation. In [1, 2], numerical methods for dealing with discontinuous source terms of singularly perturbed degenerate convection-diffusion problems were discussed. In [21], a singularly perturbed parabolic turning point with an interior layer was used. Additionally, problem (1) with a Robin boundary condition having a boundary turning point was addressed in [4, 8, 15].

Taking inspiration from the above works, we have designed a scheme which uses a uniform mesh to solve problem (1). The scheme involves the Crank-Nicolson scheme for time and a fitted operator FDM for space discretization. The objective of this work is to develop a numerical scheme that is more

accurate, stable, and uniformly convergent in solving problem (1).

Notations: Throughout this paper, the generic constant $C > 0$ is not depends on Δs, Δt and ε; the maximum norm $\|.\|$ is denoted by $\|g\|_D = \max_{(s,t)\in D} |g(s,t)|$.

2 A priori estimates

Taking $\varepsilon = 0$ in (1), we get the reduced problem

$$\begin{cases} a(s)z_s^0(s,t) - b(s,t)z_t^0(s,t) - e(s,t)z^0(s,t) = g(s,t), \ \ (s,t) \in D, \\ z^0(1,t) = \psi_r(t), \ t \in (0,T], \\ z^0(s,t) = \psi_b(s,t), \ (s,t) \in \eta_b, \end{cases} \tag{2}$$

which is a first-order hyperbolic PDE. For $a(0) = 0$ and $e(0,t) > 0$ the boundary $s = 0$ is a characteristic curve of (2), and the solution of (1) has a parabolic boundary layer closes to $s = 0$.

The next lemma will help us in determining the bound of $z(s,t)$ and its derivatives. The solution of (1) fulfils the next lemma.

Lemma 1. *(Minimum principle) Assume that $z(s,t) \in C^2(D) \cap C^0(\bar{D})$, satisfying $z(s,t) \geq 0, \ (s,t) \in \eta$. If $\mathscr{L}z(s,t) \leq 0, \ (s,t) \in D$, then $z(s,t) \geq 0, (s,t) \in \bar{D}$.*

Proof. Let $\exists (s^*,t^*) \in \bar{D}$ such that $z(s^*,t^*) = \min_{(s,t)\in\bar{D}} z(s,t) < 0$. From the supposition, we have $(s^*,t^*) \notin \{0,1\} \times \{0,T\}$ implies that (s^*,t^*) in $(0,1) \times (0,T)$. Since $z(s^*,t^*) = \min_{(s,t)\in\bar{D}} z(s,t) < 0$, then we have $z_s(s^*,t^*) = 0$, $z_t(s^*,t^*) = 0$ and $z_{ss}(s^*,t^*) \geq 0$. So that, $\mathscr{L}z(s^*,t^*) = z_{ss}(s^*,t^*) + a(s)z_s(s^*,t^*) - b(s,t)z_t(s^*,t^*) - e(s,t)z(s^*,t^*) > 0$, which is a contradiction. Therefore, $z(s,t) \geq 0, \ \forall (s,t) \in \bar{D}$. □

Lemma 2. *[3] (Stability estimate) The solution of (1) fulfills the estimate*

$$\|z\|_{\bar{D}} \leq \|z\|_{\eta} + \frac{T}{\beta}\|g\|_{\bar{D}}, \tag{3}$$

where $0 < \beta \leq b(s,t)$.

Lemma 3. *[13, 14] Let the solution of (1) be $z(s,t)$, then the derivative of $z(s,t)$ satisfies the estimate*

$$\left\| \frac{\partial^{l+j} z}{\partial s^j \partial t^l} \right\|_{\bar{D}} \leq C(1 + \varepsilon^{-j/2} \exp(-s\sqrt{\gamma/\varepsilon})), \ (s,t) \in \bar{D}, \ 1 \leq j + 2l \leq 4, \tag{4}$$

where $0 < \gamma \leq e(s,t)$.

3 The proposed method

3.1 The time semi-discretization

We use the Crank-Nicolson scheme to discretize problem (1) in the temporal direction on a uniform mesh. We define a uniform partition of $[0,T]$ with step length Δt as $\bar{D}_t^M = \{t_0 = 0, \ t_k = t_0 + k\Delta t, \ k =$

$1(1)M-1, t_M = T,\ \Delta t = T/M\}$ which has M mesh points. Then the semi-discrete result of problem (1) yields

$$\begin{cases} (\frac{\Delta t}{2}\mathscr{L}^{\Delta t} - 1)Z^{k+1}(s) = -(1+\frac{\Delta t}{2}\mathscr{L}^{\Delta t})Z^{k}(s) + \frac{\Delta t}{2}(g(s,t_k)+g(s,t_{k+1})) \\ Z^{k+1}(0) = \psi_l(t_{k+1}),\ \ Z^{k+1}(1) = \psi_r(t_{k+1}), \end{cases} \tag{5}$$

where $\mathscr{L}^{\Delta t}Z^{k+1}(s) = \varepsilon\frac{d^2Z^{k+1}(s)}{ds^2} + a(s)\frac{dZ^{k+1}(s)}{ds} - e(s,t_{k+1})Z^{k+1}(s)$.

The approximation of $Z(s,t_{k+1})$ is denoted by $Z^{k+1}(s)$ at the $(k+1)^{th}$ time level. The operator $(\frac{\Delta t}{2}\mathscr{L}^{\Delta t} - 1)Z^{k+1}(s)$ satisfies the next minimum principle.

Lemma 4. *(Semi-discrete minimum principle) Let $Z^{k+1}(s) \in C^2(\bar{D})$ such that $Z^{k+1}(0) \geq 0, Z^{k+1}(1) \geq 0$, and $(\frac{\Delta t}{2}\mathscr{L}^{\Delta t} - 1)Z^{k+1}(s) \leq 0$ on D. Then $Z^{k+1}(s) \geq 0$ on $\bar{D}$.*

Proof. Assume $\exists s^* \in \bar{D}$ such that $Z^{k+1}(s^*) = \min_{s\in\bar{D}} Z^{k+1}(s) < 0$. From the assumption, we have $s^* \notin \{0,1\}$ implies that $s^* \in (0,1)$. Since $Z^{k+1}(s^*) = \min_{s\in\bar{D}} Z^{k+1}(s) < 0$, then we have $\frac{d}{ds}Z^{k+1}(s^*) = 0$ and $\frac{d^2}{ds^2}Z^{k+1}(s^*) \geq 0$. So, the operator gives that $(\frac{\Delta t}{2}\mathscr{L}^{\Delta t} - 1)Z^{k+1}(s^*) \geq 0$, which is a contradiction to the assumption. Therefore, $Z^{k+1}(s) \geq 0, \forall s \in \bar{D}$. □

At each time step, the local truncation error for time discretization is calculated as follows: $e_{k+1}(s) := z(s,t_{k+1}) - Z^{k+1}(s)$, $k = 0(1)M$. Here, $Z^{k+1}(s)$ represents the solution obtained after one step of the semi-discrete scheme by using the exact value $z(x,t_k)$ as the starting value instead of $z^k(s)$.

Lemma 5. *If $\left|\frac{\partial^l z(s,t)}{\partial t^l}\right| \leq C,\ \ (s,t) \in \bar{D}$ and $0 \leq l \leq 2$, then the temporal direction local truncation error is bounded by*

$$\|e_{k+1}\| \leq C_1(\Delta t)^3. \tag{6}$$

The global error at t_{k+1} satisfies the bound

$$\|E_{k+1}\| \leq C(\Delta t)^2, \quad k = 1(1)M-1. \tag{7}$$

Proof. One can refer to [14] for the proof of the local truncation error bound. By using (6) up to the $(k+1)^{th}$ time step, we can obtain the global error bound at the $(k+1)^{th}$ time level:

$$\begin{aligned} \|E_{k+1}\| = \left\|\sum_{l=1}^{k+1} e_l\right\| &\leq \sum_{l=1}^{k+1}\|e_l\| \\ &\leq C_1T(\Delta t)^2, \ \text{ since } \ (k+1)\Delta t \leq T \\ &= C(\Delta t)^2, \ \ \text{where } \ C_1T = C, \end{aligned}$$

where C is not depends on ε and Δt [14]. □

Lemma 6. *[13, 14] For $k = 0(1)M-1$, the derivatives of the solution (5) satisfies the estimate*

$$\left|\frac{d^jZ^{k+1}(s)}{ds^j}\right| \leq C(1+\varepsilon^{-j/2}\exp(-s\sqrt{\gamma/\varepsilon})), \quad s \in \bar{D},\ 0 \leq j \leq 4. \tag{8}$$

Proof. To bound the derivatives of the solution (5) with respect to the spatial variable, we consider the cases for $j = 0,1,2,3,4$. For $j = 0$, it implies $|Z^{k+1}(s)| < C$. For $j = 1$, by using the argument of [19], construct a neighborhood of $I = (0, \sqrt{\varepsilon})$, $\forall s \in I$. For some $s^* \in I$ by the mean value theorem, it becomes

$$Z_s^{k+1}(s^*) = \frac{Z^{k+1}(\sqrt{\varepsilon}) - Z^{k+1}(0)}{\sqrt{\varepsilon}}. \tag{9}$$

From (9), we have

$$|Z_s^{k+1}(s^*)| = \left| \frac{Z^{k+1}(\sqrt{\varepsilon}) - Z^{k+1}(0)}{\sqrt{\varepsilon}} \right| = \varepsilon^{-1/2} |Z^{k+1}(\sqrt{\varepsilon}) - Z^{k+1}(0)| \le C\varepsilon^{-1/2} \|Z\|. \tag{10}$$

For $s \in \bar{I}$,

$$\begin{aligned} |Z_s^{k+1}(s)| &= |Z_s^{k+1}(s^*) + Z_s^{k+1}(s) - Z_s^{k+1}(s^*)| \\ &= |Z_s^{k+1}(s^*) + \int_{s^*}^{s} Z_{ss}^{k+1}(x)dx| \\ &\le |Z_s^{k+1}(s^*)| + |\varepsilon^{-1} \int_{s^*}^{s} (g(x,t_{k+1}) - a(x)Z_s^{k+1}(x) + e(s,t_{k+1})Z^{k+1}(x))dx|, \\ &\le |Z_s^{k+1}(s^*)| + C\varepsilon^{-1} \int_{s^*}^{s} (\|Z\| + \|g\|)dx = |Z_s^{k+1}(s^*)| + C\varepsilon^{-1}(\|Z\| + \|g\|)\varepsilon^{1/2}. \end{aligned} \tag{11}$$

Inserting (10) into (11), we get

$$|Z_s^{k+1}(s)| \le C\varepsilon^{-1/2} \le C(1 + \varepsilon^{-1/2} \exp(-s/\sqrt{\gamma/\varepsilon})).$$

For $j = 1$, the process is done. For $j > 1$, the higher order derivatives up to the fourth order can be obtained through induction and repeated differentiation. □

3.2 The spatial discretization

We have divided the space domain $[0,1]$ into N equal points, denoted by $s_i = ih$, where $0 \le i \le N$. The mesh spacing, which is the distance between two adjacent points, is given by $h = s_{i+1} - s_i$. The set of all these points is represented by $\bar{D}_s^N = \{0 = s_0, s_1, ..., s_N = 1,\ s_i = ih\}$. Furthermore, the divided differences operator can be expressed as follows:

$$\begin{aligned} &\delta_s^+ Z_i^k = \frac{Z_{i+1}^k - Z_i^k}{h},\ \ \delta_s^- Z_i^k = \frac{Z_i^k - Z_{i-1}^k}{h},\ \ \delta_s^0 Z_i^k = \frac{Z_{i+1}^k - Z_{i-1}^k}{2h}, \\ &\delta_s^2 Z_i^k = \frac{Z_{i-1}^k - 2Z_i^k + Z_{i+1}^k}{h^2}. \end{aligned} \tag{12}$$

Applying the central finite difference scheme in (5), for $i = 1(1)N-1$, we get

$$\begin{cases} (\frac{\Delta t}{2}\mathscr{L}^{\Delta t,h} - 1)Z_i^{k+1} = -(1 + \frac{\Delta t}{2}\mathscr{L}^{\Delta t,h})Z_i^k + \frac{\Delta t}{2}(g(s_i,t_k) + g(s_i,t_{k+1})), \\ Z^{k+1}(0) = \psi_l(t_{k+1}),\ \ Z^{k+1}(1) = \psi_r(t_{k+1}), \end{cases} \tag{13}$$

where $\mathscr{L}^{\Delta t,h}Z_i^{k+1} = \varepsilon\delta_s^2 Z_i^{k+1} + a(s_i)\delta_s^0 Z_i^{k+1} - e(s_i,t_{k+1})Z_i^{k+1}$. We use an exponential fitting factor to handle the impact of ε on spatial discretization. According to the theory of singular perturbation outlined in [16], the zero-order asymptotic solution to problem (5) at s_i can be expressed as:

$$Z^{k+1}(s_i) = Z^{k+1}(ih) = Z_0^{k+1}(ih) + (Z^{k+1}(0) - Z_0^{k+1}(0))\exp\big(-\frac{a(s_i)}{\varepsilon}ih\big), \tag{14}$$

where Z_0^{k+1} is the reduced problem solution. To manage the influence of ε, the exponentially fitting factor $\sigma(\rho)$ is introduced as

$$\mathscr{L}_\sigma^{\Delta t,h}Z_i^{k+1} = \varepsilon\sigma(\rho)\delta_s^2 Z_i^{k+1} + a(s_i)\delta_s^0 Z_i^{k+1} - e(s_i,t_{k+1})Z_i^{k+1}. \tag{15}$$

Putting $\rho = \frac{h}{\varepsilon}$ and multiplying both side by h and taking the limit as h approaches zero, we get

$$\lim_{h\to 0}\frac{\sigma(\rho)}{\rho}(Z_{i-1}^{k+1} - 2Z_i^{k+1} + Z_{i+1}^{k+1}) + a(s_i)\frac{Z_{i+1}^{k+1} - Z_{i-1}^{k+1}}{2} = 0, \tag{16}$$

which gives the variable fitting factor

$$\sigma(\rho) = \frac{\rho a(s_i)}{2}\coth\left(\frac{\rho a(s_i)}{2}\right). \tag{17}$$

3.2.1 The discrete difference scheme

Applying the central finite difference method and the fitting factor $\sigma(\rho)$, for $i = 1(1)N-1$, and $k = 0(1)M-1$, we have the following fully discrete scheme

$$\begin{cases} (\frac{\Delta t}{2}\mathscr{L}_\sigma^{\Delta t,h} - 1)Z_i^{k+1} = -(1 + \frac{\Delta t}{2}\mathscr{L}_\sigma^{\Delta t,h})Z_i^k + \frac{\Delta t}{2}(g(s_i,t_k) + g(s_i,t_{k+1})), \\ Z^{k+1}(0) = \psi_l(t_{k+1}),\ \ Z^{k+1}(1) = \psi_r(t_{k+1}), \end{cases} \tag{18}$$

where $\mathscr{L}_\sigma^{\Delta t,h}Z_i^{k+1} = \varepsilon\sigma(\rho)\delta_s^2 Z_i^{k+1} + a(s_i)\delta_s^0 Z_i^{k+1} - e(s_i,t_{k+1})Z_i^{k+1}$. We rewrite in an explicit form as

$$Q_i^- Z_{i-1}^{k+1} + Q_i^0 Z_i^{k+1} + Q_i^+ Z_{i+1}^{k+1} = R_i^- Z_{i-1}^k + R_i^0 Z_i^k + R_i^+ Z_{i+1}^k + \Delta t g(s_i, t_{k+\frac{1}{2}}), \tag{19}$$

where

$$\begin{aligned} Q_i^- &= \frac{\Delta t}{2}\left(\frac{\varepsilon\sigma(\rho)}{h^2} - \frac{a(s_i)}{2h}\right), \\ Q_i^0 &= -\frac{\Delta t\varepsilon\sigma(\rho)}{h^2} - \left(\frac{\Delta t}{2}e(s_i,t_{k+1}) + 1\right), \\ Q_i^+ &= \frac{\Delta t}{2}\left(\frac{\varepsilon\sigma(\rho)}{h^2} + \frac{a(s_i)}{2h}\right), \end{aligned} \tag{20}$$

and

$$\begin{aligned} R_i^- &= -\frac{\Delta t}{2}\left(\frac{\varepsilon\sigma(\rho)}{h^2} - \frac{a(s_i)}{2h}\right), \\ R_i^0 &= \frac{\Delta t\varepsilon\sigma(\rho)}{h^2} + \left(\frac{\Delta t}{2}e(s_i,t_k) - 1\right), \\ R_i^+ &= -\frac{\Delta t}{2}\left(\frac{\varepsilon\sigma(\rho)}{h^2} - \frac{a(s_i)}{2h}\right), \\ H_i &= \frac{\Delta t}{2}\left(g(s_i,t_k) + g(s_i,t_{k+1})\right). \end{aligned} \tag{21}$$

4 Error analysis

In this part, we study the stability and uniform convergence for the developed scheme of (18).

Lemma 7. *(Comparison principle) Assume a comparison function v_i^{k+1} such that $(\frac{\Delta t}{2}\mathscr{L}_\sigma^{\Delta t,h} - 1)Z_i^{k+1} \leq (\frac{\Delta t}{2}\mathscr{L}_\sigma^{\Delta t,h} - 1)v_i^{k+1}$ for $1 \leq i \leq N-1$ and if $Z_0^{k+1} \leq v_0^{k+1}$ and $Z_N^{k+1} \leq v_N^{k+1}$. Then $Z_i^{k+1} \leq v_i^{k+1}$ for $0 \leq i \leq N$.*

Proof. The operator $\mathscr{L}_\sigma^{\Delta t,h}Z_i^{k+1}$ with the size of matrix $(N+1)\times(N+1)$ for the entries $i = 1,2,...,N-1$ are Q_i^-, Q_i^0, and Q_i^+. We observe that $|Q_i^-| > 0$, $|Q_i^0| > 0$, $|Q_i^+| > 0$ and $|Q_i^0| \geq |Q_i^-| + |Q_i^+|$, implying that it is diagonally dominant. Then, it fulfils the criteria of the M-matrix. Thus, the inverse matrix exists and is non-negative. So, it ensures the existence of a unique discrete solution [9, 18, 20]. □

Lemma 8. *(Discrete minimum principle) Assume a function $Z(s_i,t_{k+1})$ defined on the discretized domain $\bar{D}^{N,M} = \bar{D}_s^N \times \bar{D}_t^M$. If $Z(s_i,t_{k+1}) \geq 0$, $(s_i,t_{k+1}) \in \eta^{N,M} = \bar{D}^{N,M} \cap \eta$ and $(\frac{\Delta t}{2}\mathscr{L}_\sigma^{\Delta t,h} - 1)Z(s_i,t_{k+1}) \leq 0$, $(s_i,t_{k+1}) \in D^{N,M}$, then $Z(s_i,t_{k+1}) \geq 0$, $(s_i,t_{k+1}) \in \bar{D}^{N,M}$.*

Proof. Assume $\exists (s_i^*,t_{k+1}^*) \in \bar{D}^{N,M}$ such that $Z(s_i^*,t_{k+1}^*) = \min_{(s_i,t_{k+1})\in\bar{D}} Z(s_i,t_{k+1}) < 0$. From the assumption, $(s_i^*,t_{k+1}^*) \notin \eta^{N,M}$ implies that $(s_i^*,t_{k+1}^*) \in (0,1)\times(0,T)$. Since $Z(s_i^*,t_{k+1}^*) = \min_{(s_i,t_{k+1})\in\bar{D}} Z(s_i,t_{k+1}) < 0$, then we have $Z_s(s_i^*,t_{k+1}^*) = 0$, $Z_t(s_i^*,t_{k+1}^*) = 0$ and $Z_{ss}(s_i^*,t_{k+1}^*) \geq 0$. So that, $(\frac{\Delta t}{2}\mathscr{L}_\sigma^{\Delta t,h} - 1)Z(s_i,t_{k+1}) > 0$, which is a contradiction. Therefore, $Z(s_i,t_{k+1}) \geq 0$, $(s_i,t_{k+1}) \in \bar{D}^{N,M}$. □

Lemma 9. *(Stability result) Let Z_i^{k+1} be the solution of (18), then we have*

$$\left|Z_i^{k+1}\right| \leq \frac{\| \mathscr{L}_\sigma^{\Delta t,h}Z_i^{k+1}\|}{\gamma} + \max\{|\psi_l(t_{k+1})|, |\psi_r(t_{k+1})|\},$$

where $e(s,t) \geq \gamma > 0$.

Proof. Let $P = \frac{\| \mathscr{L}_\sigma^{\Delta t,h}Z_i^{k+1}\|}{\gamma} + \max\{|\psi_l(t_{k+1})|, |\psi_r(t_{k+1})|\}$ and set the barrier functions $\theta_{i,k+1}^\pm$ by $P \pm Z_i^{k+1}$. On the boundaries, we obtain

$$\begin{aligned} \theta_{0,k+1}^\pm &= P \pm Z_0^{k+1} = \frac{\| \mathscr{L}_\sigma^{\Delta t,h}Z_i^{k+1}\|}{\gamma} + \max\{|\psi_l(t_{k+1})|, |\psi_r(t_{k+1})|\} \pm \psi_l(t_{k+1}) \geq 0, \\ \vartheta_{N,k+1}^\pm &= P \pm Z_N^{k+1} = \frac{\| \mathscr{L}_\sigma^{\Delta t,h}Z_i^{k+1}\|}{\gamma} + \max\{|\psi_l(t_{k+1})|, |\psi_r(t_{k+1})|\} \pm \psi_r(t_{k+1}) \geq 0. \end{aligned}$$

For the discretized domain s_i, $i = 1(1)N-1$, then

$$\begin{aligned}
\left(\frac{\Delta t}{2}\mathscr{L}_{\sigma}^{\Delta t,h}-1\right)\theta_{i,k+1}^{\pm} &= \frac{\Delta t}{2}\mathscr{L}_{\sigma}^{\Delta t,h}\theta_{i,k+1}^{\pm}-\theta_{i,k+1}^{\pm}\\
&=\frac{\Delta t}{2}\varepsilon\sigma(\rho)\left(\frac{P\pm Z_{i-1}^{k+1}-2(P\pm Z_i^{k+1})+P\pm Z_{i+1}^{k+1}}{h^2}\right)+\frac{\Delta t}{2}a(s_i)\left(\frac{P\pm Z_{i+1}^{k+1}-(P\pm Z_{i-1}^{k+1})}{2h}\right)\\
&\quad-\frac{\Delta t}{2}e(s_i,t_{k+1})\left(P\pm Z_i^{k+1}\right)-\left(P\pm Z_i^{k+1}\right)\\
&=\pm\frac{\Delta t}{2}\varepsilon\sigma(\rho)\left(\frac{Z_{i-1}^{k+1}-2Z_i^{k+1}+Z_{i+1}^{k+1}}{h^2}\right)\pm\frac{\Delta t}{2}a(s_i)\left(\frac{Z_{i+1}^{k+1}-Z_{i-1}^{k+1}}{2h}\right)\\
&\quad\pm\left(-\frac{\Delta t}{2}e(s_i,t_{k+1})-1\right)Z_i^{k+1}-\left(\frac{\Delta t}{2}e(s_i,t_{k+1})+1\right)P\\
&=\pm\left(\frac{\Delta t}{2}\mathscr{L}_{\sigma}^{\Delta t,h}-1\right)Z_i^{k+1}-\left(\frac{\Delta t}{2}e(s_i,t_{k+1})+1\right)P\\
&=\pm\Delta t g(s_i,t_{k+\frac{1}{2}})-\left(\frac{\Delta t}{2}e(s_i,t_{k+1})+1\right)\frac{\|\mathscr{L}_{\sigma}^{\Delta t,h}Z_i^{k+1}\|}{\gamma}+\max\{|\psi_l(t_{k+1})|,|\psi_r(t_{k+1})|\}\le 0.
\end{aligned}$$

By applying the discrete minimum principle, we can conclude that $\theta_{i,k+1}^{\pm}\ge 0$ for $i=0(1)N$. Therefore, we have obtained the desired bounds. □

Next, we determine the truncation error in the spatial direction in considering the sem-discrete scheme of (5) and the fully discrete scheme of (18).

Theorem 1. *Let the coefficient functions $a(s)$ and $e(s,t_{k+1})$ of (5) be sufficiently smooth so that $Z^{k+1}(s)\in C^4[0,1]$. Then, the solution Z_i^{k+1} of (18) fulfills the following truncation error estimate*

$$|\mathscr{L}_{\sigma}^{\Delta t,h}(Z^{k+1}(s_i)-Z_i^{k+1})|\le\frac{Ch^2}{h+\varepsilon}\left(1+\varepsilon^{-3/2}\exp(-s_i\sqrt{\gamma/\varepsilon})\right). \tag{22}$$

Proof. The estimate in the space direction is expressed as

$$\begin{aligned}
\left|\mathscr{L}_{\sigma}^{\Delta t,h}(Z^{k+1}(s_i)-Z_i^{k+1})\right| &= \left|\varepsilon(\frac{d^2}{ds^2}-\sigma(\rho)\delta_s^2)Z^{k+1}(s_i)+a(s_i)(\frac{d}{ds}-\delta_s^0)Z^{k+1}(s_i)\right|\\
&\le \left|\varepsilon(a(s_i)\frac{\rho}{2}\coth(a(s_i)\frac{\rho}{2})-1)\delta_s^2Z^{k+1}(s_i)\right|+\left|\varepsilon(\frac{d^2}{ds^2}-\delta_s^2)Z^{k+1}(s_i)\right|\\
&\quad+\left|a(s_i)(\frac{d}{ds}-\delta_s^0)Z^{k+1}(s_i)\right|,
\end{aligned} \tag{23}$$

where $\sigma(\rho)=a(s_i)\frac{\rho}{2}\coth(a(s_i)\frac{\rho}{2})$ and $\rho=\frac{h}{\varepsilon}$.

Given C_1 and C_2 are constants, then $|\rho\coth(\rho)-1|\le C_1\rho^2$, for $\rho=h/\varepsilon\le 1$. For $h/\varepsilon\to\infty$, since $\lim_{h/\varepsilon\to\infty}\coth(h/\varepsilon)=1$ which gives $|h/\varepsilon\coth(h/\varepsilon)-1|\le C_1h/\varepsilon$. Generally, $\forall\rho>0$ we express as

$$C_1\frac{\rho^2}{\rho+1}\le\rho\coth(\rho)-1\le C_2\frac{\rho^2}{\rho+1}, \tag{24}$$

thus, we get

$$\varepsilon\big(a(s_i)\frac{\rho}{2}\coth(a(s_i)\frac{\rho}{2})-1\big)\le\varepsilon\frac{(h/\varepsilon)^2}{h/\varepsilon+1}=\frac{h^2}{h+\varepsilon}. \tag{25}$$

From Taylor's series expansion, we get the bound

$$\begin{aligned}
&\left|\delta_s^2 Z^{k+1}(s_i)\right|\le C\left\|\frac{d^2}{ds^2}Z^{k+1}(s_i)\right\|,\\
&\left|(\frac{d}{ds}-\delta_s^0)Z^{k+1}(s_i)\right|\le Ch^2\left\|\frac{d^3}{ds^3}Z^{k+1}(s_i)\right\|,\\
&\left|(\frac{d^2}{ds^2}-\delta_s^2)Z^{k+1}(s_i)\right|\le Ch^2\left\|\frac{d^4}{ds^4}Z^{k+1}(s_i)\right\|.
\end{aligned} \tag{26}$$

Substituting equations (25) and (26) into (23), we get

$$\left|\mathscr{L}_\sigma^{\Delta t,h}(Z^{k+1}(s_i)-Z_i^{k+1})\right|\le\frac{Ch^2}{h+\varepsilon}\left\|\frac{d^2}{ds^2}Z^{k+1}(s_i)\right\|+Ch^2\left(\left\|\frac{d^3}{ds^3}Z^{k+1}(s_i)\right\|+\varepsilon\left\|\frac{d^4}{ds^4}Z^{k+1}(s_i)\right\|\right). \tag{27}$$

Using (8), we have the bound for the derivatives

$$\begin{aligned}
|\mathscr{L}_\sigma^{\Delta t,h}(Z^{k+1}(s_i)-Z_i^{k+1})|\le\ &\frac{Ch^2}{h+\varepsilon}\left(1+\varepsilon^{-1}\exp(-s_i\sqrt{\gamma/\varepsilon})\right)\\
&+Ch^2\left((1+\varepsilon^{-3/2}\exp(-s_i\sqrt{\gamma/\varepsilon}))+(\varepsilon+\varepsilon^{-1}\exp(-s_i\sqrt{\gamma/\varepsilon}))\right).
\end{aligned} \tag{28}$$

Evidently, $\varepsilon^{-3/2}\ge\varepsilon^{-1}$, so

$$|\mathscr{L}_\sigma^{\Delta t,h}(Z^{k+1}(s_i)-Z_i^{k+1})|\le\frac{Ch^2}{h+\varepsilon}\left(1+\varepsilon^{-3/2}\exp(-s_i\sqrt{\gamma/\varepsilon})\right), \tag{29}$$

thus, we get the wanted bounds. □

Lemma 10. *[15] For a fixed N mesh numbers and as $\varepsilon\to 0$, we obtain*

$$\lim_{\varepsilon\to 0}\max_i\frac{\exp(-s_i\sqrt{\gamma/\varepsilon})}{\varepsilon^{j/2}}=0,\quad j=1,2,3,\ldots, \tag{30}$$

where $s_i=ih$, $i=1(1)N-1$.

Theorem 2. *Let the solution of (18) be Z_i^{k+1}, then the uniform error is estimated by*

$$\sup_{\varepsilon\in(0,1]}\max_i|Z^{k+1}(s_i)-Z_i^{k+1}|\le Ch, \tag{31}$$

where $i=0(1)N$.

Proof. Plugging (30) into (22), we get

$$|\mathscr{L}_{\sigma}^{\Delta t,h}(Z^{k+1}(s_i)-Z_i^{k+1})| \leq \frac{Ch^2}{h+\varepsilon}. \tag{32}$$

Hence, the result leads to $|Z^{k+1}(s_i)-Z_i^{k+1}| \leq \frac{Ch^2}{h+\varepsilon}$. Using the sup overall $\varepsilon \in (0,1]$, we get

$$\sup_{\varepsilon\in(0,1]} \max_i |Z^{k+1}(s_i)-Z_i^{k+1}| \leq Ch. \tag{33}$$

When the step size is less than ε, the method provides second-order convergence. For step sizes much larger than ε, the method provides first-order convergence. □

Theorem 3. *Let z and Z be the solutions of (1) and (18), respectively. Then, the uniform error estimate for the fully discrete scheme is given by*

$$\sup_{\varepsilon\in(0,1]} |z-Z| \leq C(h+(\Delta t)^2). \tag{34}$$

Proof. The proof follows by combining (31) and (7). □

5 Numerical experiments

We applied the proposed scheme to two examples to support our theoretical findings. Since we do not have exact solutions for these examples, we used the double mesh principle to calculate the maximum absolute error. The computation of the maximum absolute error is given by $E_{\varepsilon}^{N,M} = \max_{i,k} |Z_{i,k}^{N,M} - Z_{i,k}^{2N,2M}|$. The ε-uniform error is estimated by finding the maximum of all the maximum absolute errors and is given by $E^{N,M} = \max_{i,k}(E_{\varepsilon}^{N,M})$. We estimate the order of convergence by $r_{\varepsilon}^{N,M} = \log_2(E_{\varepsilon}^{N,M}/E_{\varepsilon}^{2N,2M})$. The ε-uniform order of convergence is estimated by $r^{N,M} = \log_2(E^{N,M}/E^{2N,2M})$.

Example 1. Consider

$$\begin{cases} \varepsilon\frac{\partial^2 z}{\partial s^2} + s^p\frac{\partial z}{\partial s} - z - \frac{\partial z}{\partial t} = s^2-1,\ (s,t)\in(0,1)\times(0,1], \\ z(s,0) = (1-s)^2,\ s\in\bar{D}, \\ z(0,t) = 1+t^2,\ z(1,t) = 0,\ t\in(0,1]. \end{cases}$$

Example 2. Consider

$$\begin{cases} \varepsilon\frac{\partial^2 z}{\partial s^2} + s^p\frac{\partial z}{\partial s} - (s+p)z - \frac{\partial z}{\partial t} = p(s^2-1)exp(-t),\ (s,t)\in(0,1)\times(0,1], \\ z(s,0) = (1-s)^2,\ s\in\bar{D}, \\ z(0,t) = 1+t^2,\ z(1,t) = 0,\ t\in(0,1]. \end{cases}$$

We computed $E_{\varepsilon}^{N,M}$, $E^{N,M}$ and $r^{N,M}$ for each example using the developed scheme (18). The obtained results for the model Examples 1 and 2 for distinct values of ε and N are displayed in Tables 1 and 3, respectively. These results show that for every value of ε, the maximum absolute error decreases as the step sizes decrease. Also we observed that the maximum absolute error becomes constant as ε gets smaller, which indicates ε-uniform convergence of the proposed scheme, regardless of ε. The results in

Table 1: $E_{\varepsilon}^{N,M}, E^{N,M}$ and $r^{N,M}$ of Example 1 for $p = 1$.

	Number of intervals $N = M$			
$\varepsilon \downarrow$	32	64	128	256
10^{-6}	8.0607e-03	4.4718e-03	2.4120e-03	1.2744e-03
10^{-8}	8.0607e-03	4.4718e-03	2.4120e-03	1.2744e-03
10^{-10}	8.0607e-03	4.4718e-03	2.4120e-03	1.2744e-03
10^{-12}	8.0607e-03	4.4718e-03	2.4120e-03	1.2744e-03
10^{-16}	8.0607e-03	4.4718e-03	2.4120e-03	1.2744e-03
10^{-18}	8.0607e-03	4.4718e-03	2.4120e-03	1.2744e-03
10^{-20}	8.0607e-03	4.4718e-03	2.4120e-03	1.2744e-03
$E^{N,M}$	8.0607e-03	4.4718e-03	2.4120e-03	1.2744e-03
$r^{N,M}$	0.8501	0.8906	0.9204	-

Table 2: Comparison of $E^{N,M}$ and $r^{N,M}$ for Example 1 and results in [10] for $p = 1$.

		Number of intervals $N = M$			
Schemes $\downarrow$		32	64	128	256
Proposed scheme	$E^{N,M}$	8.0607e-03	4.4718e-03	2.4120e-03	1.2744e-03
	$r^{N,M}$	0.8501	0.8906	0.9204	-
Results in [10]	$E^{N,M}$	3.0430e-02	1.1938e-02	6.1610e-03	3.2113e-03
	$r^{N,M}$	1.3499	0.9543	0.9400	0.9599

Table 3: $E_{\varepsilon}^{N,M}, E^{N,M}$ and $r^{N,M}$ of Example 2 for $p = 1$.

	Number of intervals $N = M$			
$\varepsilon \downarrow$	32	64	128	256
10^{-6}	5.8935e-03	3.1304e-03	1.6083e-03	8.1279e-04
10^{-8}	5.8935e-03	3.1304e-03	1.6083e-03	8.1279e-04
10^{-10}	5.8935e-03	3.1304e-03	1.6083e-03	8.1279e-04
10^{-12}	5.8935e-03	3.1304e-03	1.6083e-03	8.1279e-04
10^{-16}	5.8935e-03	3.1304e-03	1.6083e-03	8.1279e-04
10^{-18}	5.8935e-03	3.1304e-03	1.6083e-03	8.1279e-04
10^{-20}	5.8935e-03	3.1304e-03	1.6083e-03	8.1279e-04
$E^{N,M}$	5.8935e-03	3.1304e-03	1.6083e-03	8.1279e-04
$r^{N,M}$	0.9128	0.9608	0.9846	-

Table 4: Comparison of $E_\varepsilon^{N,M}$ and $r_\varepsilon^{N,M}$ for Example 2 and results in [12] for $p = 1$.

	Number of intervals $N = M$				
$\varepsilon \downarrow$	32	64	128	256	512
	Present method				
2^{-10}	5.7949e-03	3.2560e-03	2.5153e-03	1.5669e-03	8.7472e-04
	0.8317	0.3724	0.6828	0.8410	-
2^{-15}	5.8935e-03	3.1304e-03	3.8325e-03	1.7184e-03	7.1006e-04
	0.9128	-0.2919	1.1572	1.2751	-
2^{-20}	5.8935e-03	3.1304e-03	1.6083e-03	8.1279e-04	4.6537e-04
	0.9128	0.9608	0.9846	0.8045	-
2^{-25}	5.8935e-03	3.1304e-03	1.6083e-03	8.1279e-04	4.0825e-04
	0.9128	0.9608	0.9846	0.9934	-
2^{-30}	5.8935e-03	3.1304e-03	1.6083e-03	8.1279e-04	4.0825e-04
	0.9128	0.9608	0.9846	0.9934	-
	Results in [12]				
2^{-10}	1.7481e-02	1.0302e-02	5.9462e-03	3.3853e-03	1.9118e-03
	0.7629	0.7929	0.8127	0.8244	-
2^{-15}	1.6983e-02	1.0060e-02	5.8145e-03	3.3187e-03	1.8729e-03
	0.7554	0.7901	0.8090	0.8254	-
2^{-20}	1.6951e-02	1.0051e-02	5.8101e-03	3.3167e-03	1.8717e-03
	0.7540	0.7907	0.8088	0.8254	-
2^{-25}	1.6948e-02	1.0050e-02	5.8101e-03	3.3167e-03	1.8717e-03
	0.7538	0.7906	0.8088	0.8254	-
2^{-30}	1.6947e-02	1.0050e-02	5.8101e-03	3.3167e-03	1.8717e-03
	0.7538	0.7906	0.8088	0.8254	-

Table 5: $E_\varepsilon^{N,M}$ and $r_\varepsilon^{N,M}$ for $\varepsilon = 10^{-10}$.

$p \downarrow$	Example 1			Example 2		
	$N = 32$	64	128	32	64	128
	$M = 32$	64	128	32	64	128
1	8.0607e-03	4.4718e-03	2.4120e-03	5.8935e-03	3.1304e-03	1.6083e-03
	0.8501	0.8906	-	0.9128	0.9608	-
2	6.5919e-03	3.9087e-03	2.2569e-03	3.4578e-03	1.8498e-03	9.5601e-04
	0.75401	0.7924	-	0.9025	0.9523	-
3	5.6792e-03	3.4719e-03	2.0786e-03	5.0147e-03	2.7300e-03	1.4226e-03
	0.7100	0.7401	-	0.8773	0.9404	-
4	4.9951e-03	3.1524e-03	1.9183e-03	6.4596e-03	3.5805e-03	1.8817e-03
	0.6641	0.7166	-	0.8513	0.9281	-

Table 6: $E_{\varepsilon}^{N,M}$ and $r_{\varepsilon}^{N,M}$

$\varepsilon\downarrow$	Example 1			Example 2		
	$N=16$	64	256	16	64	256
	$M=16$	32	64	16	32	64
10^{-6}	1.3867e-02	4.4018e-03	1.2511e-03	1.0405e-02	3.0735e-03	7.9741e-04
	1.6555	1.8149	-	1.7593	1.9465	-
10^{-8}	1.3867e-02	4.4018e-03	1.2511e-03	1.0405e-02	3.0735e-03	7.9741e-04
	1.6555	1.8149	-	1.7593	1.9465	-
10^{-10}	1.3867e-02	4.4018e-03	1.2511e-03	1.0405e-02	3.0735e-03	7.9741e-04
	1.6555	1.8149	-	1.7593	1.9465	-
10^{-12}	1.3867e-02	4.4018e-03	1.2511e-03	1.0405e-02	3.0735e-03	7.9741e-04
	1.6555	1.8149	-	1.7593	1.9465	-

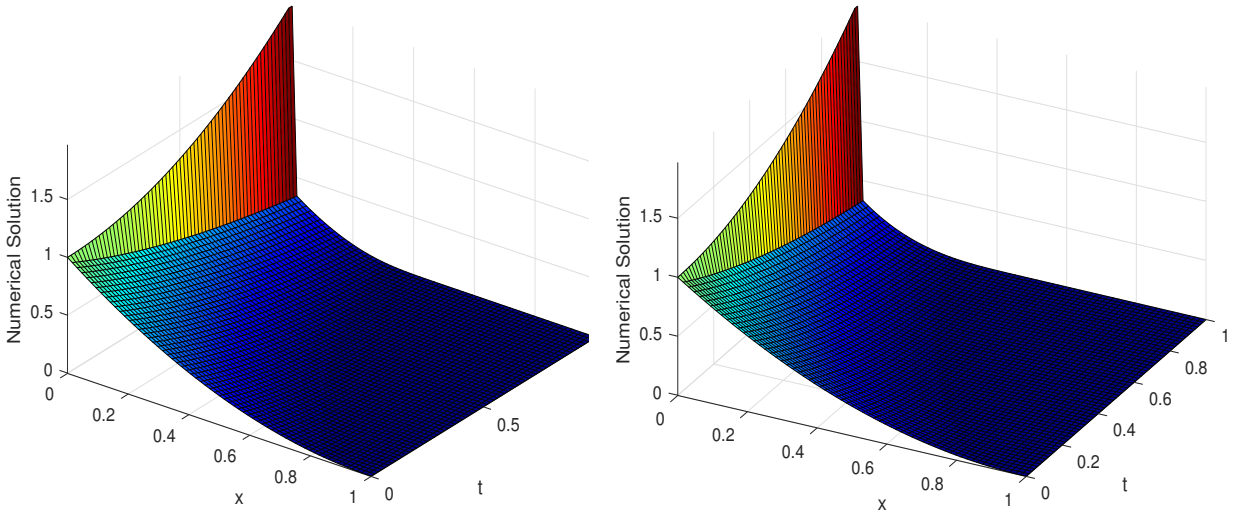

(a) Example 1 (b) Example 2

Figure 1: Numerical result surface plot with $N=M=64$, $p=1$, and $\varepsilon=10^{-20}$.

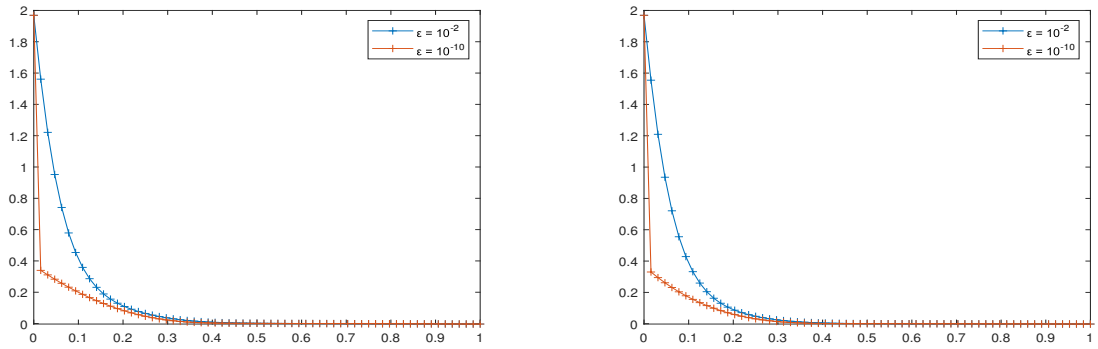

(a) Example 1 (b) Example 2

Figure 2: Computed solution with $N = M = 64$ and $p = 1$.

the last two rows of each table show that the calculated values of $E^{N,M}$ and the corresponding $r^{N,M}$, which confirms that the theoretical finding of the developed scheme is order one in space. Further, in Table 5, we provided ε-uniform pointwise error and the corresponding ε-uniform convergence for distinct values of $p \geq 1$ for the two examples. From the results, we observed that the error estimate does not depend on the values of p. Additionally, we used $4N$ and $2M$ to confirm that our scheme has order two in time and the results are delineated in Table 6. We also compared the presented scheme with some of the existing published works, as seen in Tables 2 and 4, and found that it has better accuracy.

Based on the model examples and the derivative bounds, the problem has a boundary layer near $s = 0$. Figure 1 shows the surface plot solutions of Example 1 and Example 2 for $\varepsilon = 10^{-20}$, $N = M = 64$, and $p = 1$. On the other hand, Figure 2 visualizes the numerical solution of Examples 1 and Example 2. The figures reveal a parabolic boundary layer of width $O(\sqrt{\varepsilon})$ around $s = 0$ as $\varepsilon \to 0$.

6 Conclusions

A uniformly convergent numerical scheme is constructed to solve the class of singularly perturbed parabolic turning point problem. The scheme used the Crank-Nicolson method for time and an exponentially fitted central finite difference method for space derivative. Comparison principles ensured the stability of the scheme and are used to analyze the scheme for uniform convergence. The results are demonstrated numerically by computing maximum absolute error, ε-uniform error, and ε-uniform order of convergence in tables. The experimental results agreed with the theoretical findings. The proposed method is stable, ε-uniformly convergent, with first-order in space and second-order in time. The surface plots of the numerical solution and the left boundary layer of the solution are revealed graphically.

Acknowledgements

The authors are grateful in advance to the anonymous referees and the editor for their valuable comments.

References

[1] C. Clavero, J.L. Gracia, G.I. Shishkin, L.P. Shishkina, *Grid approximation of a singularly perturbed parabolic equation with degenerating convective term and discontinuous right-hand side*, Int. J. Numer. Anal. Mod. **10** (2013).

[2] C. Clavero, J.L. Gracia, G.I. Shishkin. L.P. Shishkina, *Schemes convergent-uniformly for parabolic singularly perturbed problems with a degenerating convective term and a discontinuous source*, Math. Model. Anal. **20** (2015) 641–657.

[3] R.K. Dunne, E.O'Riordan, G.I. Shishkin, *A fitted mesh method for a class of singularly perturbed parabolic problems with a boundary turning point*, Comput. Methods Appl. Math. **3** (2003) 361–372.

[4] F.W. Gelu, G.F. Duressa, *A parameter-uniform numerical method for singularly perturbed Robin type parabolic convection-diffusion turning point problems*, Appl. Numer. Math. **190** (2023) 50–64.

[5] V. Gupta, M.K. Kadalbajoo, *A layer adaptive B-spline collocation method for singularly perturbed one-dimensional parabolic problem with a boundary turning point*, Numer. Methods Partial Differ. Equ. **27** (2011) 1143–1164.

[6] T.C. Hanks, *Model relating heat-flow values near, and vertical velocities of mass transport beneath, oceanic rises*, J. Geophys. Res. **76** (1971) 537–544.

[7] G. Janani Jayalakshmi, A.Tamilselvan, *Hybrid difference scheme for singularly perturbed convection diffusion boundary turning point problems with discontinuous source term*, Int. J. Appl. Comput. **5** (2019) 1–14.

[8] G. Janani Jayalakshmi, A. Tamilselvan, *An ε-uniform method for a class of singularly perturbed parabolic problems with Robin boundary conditions having boundary turning point*, Asian-Eur. J. Math. **13** (2020) 1–15.

[9] R.B. Kellogg, A. Tsan, *Analysis of some difference approximations for a singular perturbation problem without turning points*, Math. Comput. **32** (1978) 1025–1039.

[10] S. Kumar, Sumit, J. Vigo-Aguiar, *A parameter-uniform grid equidistribution method for singularly perturbed degenerate parabolic convection-diffusion problems*, J. Comput. Appl. Math. **404** (2020) 113273.

[11] S. Ku Sahoo, V. Gupta, *Second-order parameter-uniform finite difference scheme for singularly perturbed parabolic problem with a boundary turning point*, J. Differ. Equ. Appl. **27** (2021) 223–240.

[12] A. Majumdar, S. Natesan, *Second-order uniformly convergent Richardson extrapolation method for singularly perturbed degenerate parabolic PDEs*, Int. J. Appl. Comput. Math. **3** (2017) 31–53.

[13] A. Majumdar, S. Natesan, *An ε-uniform hybrid numerical scheme for a singularly perturbed degenerate parabolic convection-diffusion problem*, Int. J. Comput. Math. **96** (2019) 1313–1334.

[14] N.A. Mbroh, C.O. Noutchie, R.Y. Massoukou, *A second order fitted operator finite difference scheme for a singularly perturbed degenerate parabolic problem*, Int. J. Nonlinear Anal. Appl. **12** (2021) 677–687.

[15] N.A. Mbroh, C.O. Noutchie, R.Y. Massoukou, *A uniformly convergent finite difference scheme for robin type singularly perturbed parabolic convection diffusion problem*, Math. Comput. Simul. **174** (2020) 218–232.

[16] R.E. O'malley, *Singular perturbation methods for ordinary differential equations*, 89 (1991).

[17] S. Singh, D. Kumar, H. Ramos, *A uniformly convergent quadratic B-spline based scheme for singularly perturbed degenerate parabolic problems*, Math. Comput. Simul. **195** (2022) 88–106.

[18] S.K. Tesfaye, M.M. Woldaregay, T.G. Dinka, G.F. Duressa, *Fitted computational method for solving singularly perturbed small time lag problem*, BMC Res. Notes **15** (2022) 1–10.

[19] R. Vulanović, P.A. Farrell, *Continuous and numerical analysis of a multiple boundary turning point problem*, SIAM J. Numer. Anal. **30** (1993) 1400–1418.

[20] M.M. Woldaregay, W.T. Aniley, G.F. Duressa, *Novel numerical scheme for singularly perturbed time delay convection-diffusion equation*, Adv. Math. Phys. **2021** (2021) 1–13.

[21] S. Yadav, P. Rai, *An almost second order hybrid scheme for the numerical solution of singularly perturbed parabolic turning point problem with interior layer*, Math. Comput. Simul. **185** (2021) 733–753.

[22] S. Yadav, P. Rai, K. Sharma, *A higher order uniformly convergent method for singularly perturbed parabolic turning point problems*, Numer. Methods Partial Differ. Equ.**36** (2020) 342–368.